



Surface Properties of Liquid Al-Ni Alloys: Experiments Vs Theory

R. Novakovic¹ · M. Mohr² · D. Giuranno¹ · E. Ricci¹ · J. Brillo³ · R. Wunderlich⁴ · I. Egry⁵ · Yu Plevachuk⁶ · H.-J. Fecht²

Received: 23 May 2020 / Accepted: 10 September 2020 / Published online: 25 September 2020
© Springer Nature B.V. 2020

Abstract

The present study is an overview of the surface properties of liquid Al-Ni alloys, which are of great importance for the design and development of new Al-Ni and Ni-based industrial alloys, widely used as functional and structural materials. The solidification and thus, the microstructural evolution are directly dependent on the interface/surface properties of metallic melts. Therefore, numerical simulation of microstructure evolution requires reliable property data as input to such models. Taking into account the experimental difficulties related to a high reactivity of liquid Al-Ni alloys and the effects of impurities on their surface properties, the surface tension over the whole concentration range has been determined in the frameworks of three international research projects. Namely, the surface tension measurements have been carried out by both traditional container-based and as an alternative, containerless methods within the ESA-MAP ThermoProp and ESA-MAP Thermolab Projects and also under the EU FP6-IMPRESS Project. The obtained datasets were analysed and subsequently compared with the model predicted values as well as with the literature data. A strong exothermic mixing characterises the Al-Ni system and the presence of a few intermetallic compounds in the solid state leads to the formation of short range ordered elements or complexes in the liquid phase, at least near the melting temperature, which significantly affects the surface properties of alloy melts. Aiming to estimate the effects of short range ordering on these properties, the Compound Formation Model (CFM) and the Quasi Chemical Approximation (QCA) for regular solution were applied.

Keywords Al-Ni · Surface tension · Sessile/large drop methods · Parabolic flight · Electromagnetic levitation · Thermodynamics and statistical mechanics

This article belongs to the Topical Collection: The Effect of Gravity on Physical and Biological Phenomena, Guest Editor: Valentina Shevtsova

✉ R. Novakovic
rada.novakovic@ge.icmate.cnr.it

¹ Institute of Condensed Matter Chemistry and Technologies for Energy, National Research Council (CNR-ICMATE), Via de Marini 6, 16149 Genoa, Italy

² Institute of Functional Nanosystems, Ulm University, Albert-Einstein-Allee 47, 89081 Ulm, Germany

³ Institut für Materialphysik im Weltraum, Deutsches Zentrum für Luft- und Raumfahrt (DLR), 51170 Köln, Germany

⁴ Metallurgy Europe, gGmbH, Magirus-Deutz-Straße 12, 89077 Ulm, Germany

⁵ Institute of Theoretical Physics, RWTH-Aachen University, 52056 Aachen, Germany

⁶ Department of Metal Physics, Ivan Franko National University, Lviv 79005, Ukraine

Introduction

The Al-Ni system has great importance in itself and in particular as a subsystem of multicomponent Ni-based superalloys containing Cr, Co, Mo, Ta, Re, Ti, Hf and W, applied in various fields such as power generation and automotive industries, fuel cell and hydrogen technology, catalytic chemistry and protective coatings (Furrer and Fecht 1999; Ricci et al. 2007; Zeifert et al. 2008; Wunderlich and Fecht 2011; Giuranno et al. 2015; Amore et al. 2016; De et al. 2016; Cormier 2018). The presence of the $AlNi_3$ intermetallic phase, known as γ' phase, exhibiting high degree of order at high temperatures, is a key to strengthening in binary Al-Ni (Ansara et al. 1997) and multicomponent Ni-based alloys (Dupin et al. 2001). The outstanding high temperature mechanical properties of Ni-based superalloys can be attributed to the coherency between their constituting phases γ (A1) matrix and γ' ($L1_2$) hardening precipitates (the $L1_2$ structure being an ordered state of the fcc (A1) lattice), and together with good oxidation resistance make these alloys suitable for extremely harsh environments (Pollock and Tin 2006; Park et al. 2015). To produce materials with desired

properties it is necessary to understand the relationships between the elements of a quadriade “*composition-processing-microstructure-properties*” and based on it, to achieve tailored microstructure associated with a unique combination of properties (Ashby et al. 2004).

Design and development of new Al-Ni and Ni-based industrial alloys involve different processing routes reported in (Jarvis and Voss 2005; Rösler et al. 2005; Weber et al. 2016), including the most advanced such as additive manufacturing (Keller et al. 2017; Nandwana et al. 2017). Ni-based structural components are mainly produced using the traditional liquid phase route, i.e. an investment casting process (Furrer and Fecht 1999; Pollock and Tin 2006). Model simulations that allow predicting the microstructural evolution of Al-Ni and Ni-based industrial alloys during solidification can be helpful to evaluate the operating parameters, relevant for the optimization of casting processes (Wang et al. 2007). Therefore, accuracy and reliability of the thermophysical property data, used as input to numerical simulations, are relevant for both industry and basic science (Fecht 2008; Quested et al. 2009). Among the thermophysical properties such as the surface tension, viscosity, mass density, specific heat, total hemispherical emissivity, thermal conductivity, and electrical resistivity, *the surface tension* of alloy melts is the key property for the modeling of microstructure evolution during solidification. On the other side, a comparison with a real system is the most reliable and preferred way to validate a simulation model and therefore, the surface tension predictive models can be validated using the experimental surface tension data obtained by accurate and precise measurements (Egry et al. 2010).

In 1961, the surface tension of liquid Al-Ni alloys has been measured for the first time by Eremenko et al. (Eremenko et al. 1961) using the sessile drop method. Few years later, two series of measurements over the whole composition range have been performed by the large drop method: first, for temperatures ranging between 1273 and 2023 K (Ayushina et al. 1969), and second, at the temperature of $T = 1913$ K (Levin and Ayushina, 1974), giving the same results. In all cases, neither the experimental procedure nor the equipment were described in detail and therefore it was impossible to reproduce those experiments. After 2000, there were considerable scientific and industrial interests in design and development of novel metallic materials with a wide range of potential applications and relevant manufacturing methods (Weber et al. 2016). At the same time, the fast progress of computer technologies contributed to developing more sophisticated numerical models and containerless measurement methods lead to results that are more accurate. Measurements of high temperature liquid metallic materials such as Ni-based and Ti-based industrial alloys and their thermophysical properties have become the subject of paramount research interest and in the last two decades have been widely investigated in the frameworks of the three international projects. Indeed, in August 2001, the

ESA-MAP Thermolab (Microgravity Application Programme-Thermophysical Properties of Liquid Metallic Alloys for Modelling of Industrial Solidification Processes and Development of Advance Components and Products) project started with the aim to concentrate on specific experimental and theoretical aspects of thermophysical properties, including measurements in reduced gravity/microgravity conditions thanks to containerless levitation processing (Thermolab Final Report 2003; Fecht et al. 2005; Aune et al. 2006; Wunderlich and Fecht, 2011). Since 2009 the ESA-MAP ThermoProp (Microgravity Application Programme-Thermophysical Properties of Liquid Metals for Industrial Process) project activities represent the continuation of the aforementioned project extending the research to new classes of materials (bulk metallic glasses, steels, semiconductors, etc.) as well as to performing long-duration microgravity experiments on board the International Space Station (ISS) (Wunderlich et al. 2017; Mohr^{1,2} et al. 2019a, b).

Within the EU-IMPRESS (Intermetallic Materials Processing in Relation to Earth and Space Solidification) project (2004–2009), two specific families of intermetallics have been studied, namely titanium aluminides (TiAl) and nickel aluminides (NiAl) as well as multicomponent alloys based on these compositions (Jarvis and Voss 2005; IMPRESS Final Report 2009). The research activities related to the study of thermophysical properties, similar to those of the two ESA MAP projects, involved the selection of material and, depending on its physico-chemical properties, the choice of predictive models, experimental conditions as well as appropriate measurement methods. In the case of AlTi and AlNi-based alloys, the surface tension has been measured starting from conventional container-based followed by a quasi-containerless pendant drop method and finally, using advanced containerless processing techniques of hot melts on ground and under reduced gravity conditions, and the experimental data obtained were analysed using theoretical models (Egry et al. 2008; Egry^{1,2} et al. 2010a, b; Wunderlich et al. 2018).

The present paper reviews experimental and theoretical work on the surface tension of liquid Al-Ni alloys and presents the state of the art on this research topic. The surface tension datasets obtained by different measurements, the experimental methods, predictive models and their validity are discussed. The Al-Ni phase diagram indicates the presence of five intermetallic compounds. Together with the thermodynamic properties of Al-Ni alloys exhibiting pronounced negative deviations from ideality over the whole composition range as well as largely negative mixing functions (Ansara et al. 1997), this alloy system as a strongly interacting compound forming one (Singh and March 1995). Therefore, the Compound Formation Model (CFM) that takes into account the effects of short range ordering on the surface tension and surface segregation is the most appropriate one to analyse the collected Al-Ni surface tension datasets. At the same time, the Quasi

Chemical Approximation (QCA) for regular solution and Butler's model are applied to evaluate the differences between model predicted values (Aune et al. 2006; Egry² et al. 2010b).

Experimental Methods

Surface tension is very sensitive to the presence of oxygen, sulphur and other surface active elements. For instance, only a few ppm of oxygen can lead to a significant reduction of surface tension of metallic melts, by 30% and even more. This can be attributed to high chemical reactivity of liquid metals at high temperatures, principally with oxygen present in the surrounding atmosphere and, in the case of contact methods, the interfacial reactions between melt and substrate or container. To avoid or at least minimize these problems, the evaluation of the wetting behaviour of the system of interest has been done suggesting the appropriate measurement method or the possibility to limit chemical reactions (measurements out of equilibrium). In the case of extremely reactive melts, it is therefore necessary to avoid or even suppress any possible reaction of the sample with the container material and the application of the contactless methods is recommended. Otherwise, a combined thermodynamic-kinetic study of the system under investigation can indicate the experimental conditions and the physical-chemical parameters (e.g. pressure; composition of the sample itself; composition of the gaseous and solid (support) environment; vapour pressure etc.) aiming to achieve accurate and reliable surface tension data (Fecht et al. 2005; Fecht 2008; Egry² et al. 2010b).

In the following, the measurement methods used to obtain the experimental surface tension data of liquid Al-Ni alloys (Table 1) are briefly described. More information and details can be found in (Kozakevitch and Urbain 1961; Padday 1969; Defay 1971; Maze and Burnet 1971; Naidich 1981; Egry² et al. 2010b; Cummings and Blackburn 1991; Lohöfer et al. 1991; Egry 1991; Egry et al. 2005; Brillo et al. 2006; Mohr¹ et al. 2019; Lohöfer 2020).

Container-Based Methods

Sessile/Large Drop

The sessile drop is a drop shape method (Padday 1969). During the measurement a liquid drop is placed on a flat, unwetted, solid support (Fig. 1a) and its profile image is acquired. The Laplace equation (Defay 1971) describes the drop shape. Such equation has no analytical solution, so the surface tension is determined by the fitting of the experimental drop shape (Bashforth and Adams 1883), as shown in Fig. 1b. The advantage of this method is a non-invasive character and the best results are obtained for non-wetting systems (Kozakevitch and Urbain 1961), such as the metal/refractory

systems. Computerised numerical calculations and computer-aided imaging techniques allow the measurement of the shape of the drop with the highest possible precision. The recorded digital images of the drop are analysed to obtain numerical data points of its contour. Dedicated software packages are adopted to obtain surface tension data in real time together with other experimental parameters. Normally, the surface tension is calculated by using an improved version of the Maze and Burnet algorithm (Maze and Burnet 1969; Maze and Burnet 1971). In order to obtain a good accuracy, a knowledge of the magnification factor of the used system is essential for deriving the real drop profile coordinates from the acquired ones. Beyond this, other facts have to be considered in order to obtain reliable surface tension data. Some “standard criteria” both in the design of the apparatuses and in the procedures for the surface tension measurement at high temperatures, should be taking into account, such as those described in (Egry² et al. 2010b).

Large Drop

When the contact angle between the liquid metal and the support/container material is greater than 90°, a variant of the sessile drop method, based on the concept of “large drop” (Naidich 1981) and called “pinned drop method” is recommended (Egry² et al. 2010b). In this case, the solid support is a special circular crucible with sharp edges (Fig. 1c). Equilibrium drop profile and its description by means of contour fitting are shown in Fig. 1b. The design of the edges of the crucible blocks the triple line at an “apparent” contact angle that is much higher than the real one. A further advantage of the pinned drop method is that the axisymmetry of the drop can be imposed.

Containerless Measurements

EML- Oscillating Drop on Ground (OD-EML⁹)

By eliminating the contact of the melt with a container, there is no possibility of contamination with container material, which allows for measurements with a higher precision. To this end, the containerless method of the oscillating drop is typically used (Egry 1991; Egry et al. 2005). For electrically conducting materials, such as metals, despite the enormous progress that has been made with the development of electrostatic levitation, the electromagnetic levitation is still the most suitable for the containerless processing of liquid metallic materials. This is especially true for non-refractory metals and metals with a high vapour pressure. The sample is hereby levitated by an electromagnetic *rf* field inducing eddy currents inside the sample, which inductively heat the latter and position it against gravity due to Lorenz-forces.

Table 1 Parameters of the linear fits $\sigma = \sigma_0 - d\sigma/dT(T - T_L)$ to the experimental surface tension datasets for liquid Al-Ni alloys. SD-sessile drop, LD-large drop, OD-oscillating drop, EML-electromagnetic levitation, PF-parabolic flights; R-recommended values obtained

combining the results of different measurements. Superscripts: *g* – on ground, *μ-g* – microgravity. (*Equation for linear fits proposed by the authors)

Alloy composition, at %	Liquidus temperature T_L , K	Surface tension σ_0 at T_L , Nm^{-1}	Temperature coefficient $d\sigma/dT$, $10^{-4}Nm^{-1}K^{-1}$	Method	Measurement temperature/range, K	Experim. error, %
(Eremenko et al. 1961)						
Ni	–	1.718	–	SD	1913	1.0
Al _{21.5} Ni _{78.5}	–	1.543	–	SD	1913	1.0
Al _{23.9} Ni _{76.1}	–	1.508	–	SD	1913	1.0
Al _{24.9} Ni _{75.1}	–	1.568	–	SD	1913	1.0
Al _{27.9} Ni _{72.1}	–	1.511	–	SD	1913	1.0
Al _{29.5} Ni _{70.5}	–	1.464	–	SD	1913	1.0
Al _{35.6} Ni _{64.4}	–	1.476	–	SD	1913	1.0
Al _{38.8} Ni _{61.2}	–	1.487	–	SD	1913	1.0
Al _{42.8} Ni _{57.2}	–	1.437	–	SD	1913	1.0
Al _{44.7} Ni _{55.3}	–	1.464	–	SD	1913	1.0
Al _{48.2} Ni _{51.8}	–	1.477	–	SD	1913	1.0
Al _{50.9} Ni _{49.1}	–	1.393	–	SD	1913	1.0
Al _{55.2} Ni _{44.8}	–	1.306	–	SD	1913	1.0
Al _{55.7} Ni _{44.3}	–	1.274	–	SD	1913	1.0
Al _{58.1} Ni _{41.9}	–	1.289	–	SD	1913	1.0
Al _{77.5} Ni _{22.5}	–	0.979	–	SD	1913	1.0
Al _{96.7} Ni _{3.3}	–	0.809	–	SD	1913	1.0
Al _{98.6} Ni _{1.4}	–	0.834	–	SD	1913	1.0
Al	–	0.829	–	SD	1913	1.0
(Ayushina et al. 1969)						
Ni	–	2.090*	–2.20	LD	1273–2023	–
Al _{10.3} Ni _{89.7}	–	2.174*	–3.80	LD	1273–2023	–
Al _{50.4} Ni _{49.6}	–	1.772*	–1.70	LD	1273–2023	–
Al ₃ Ni ₂	–	1.534*	–1.40	LD	1273–2023	–
Al _{67.8} Ni _{32.2}	–	1.337*	–0.90	LD	1273–2023	–
Al _{76.7} Ni _{23.3}	–	1.146*	–0.80	LD	1273–2023	–
Al _{83.7} Ni _{16.3}	–	1.298*	–2.60	LD	1273–2023	–
Al _{89.6} Ni _{10.4}	–	1.107*	–1.80	LD	1273–2023	–
(Levin and Ayushina 1974)						
Ni	–	2.09*	–2.20	LD	1913	± 3.0
Al _{10.3} Ni _{89.7}	–	2.174*	–3.80	LD	1913	± 3.0
AlNi	–	1.772*	–1.70	LD	1913	± 3.0
Al ₃ Ni ₂	–	1.534*	–1.40	LD	1913	± 3.0
Al _{67.8} Ni _{32.2}	–	1.337*	–0.90	LD	1913	± 3.0
Al _{76.7} Ni _{23.3}	–	1.146*	–0.80	LD	1913	± 3.0
Al _{83.7} Ni _{16.3}	–	1.298*	–2.60	LD	1913	± 3.0
Al _{89.6} Ni _{10.4}	–	1.107*	–1.80	LD	1913	± 3.0
(Giuranno et al. 2010)						
Al _{97.6} Ni _{2.4}	913	0.830	–1.10	LD	1053–1123	± 0.5
Al _{92.5} Ni _{7.5}	1043	0.875	–1.85	LD	1123–1233	± 0.5
Al _{89.7} Ni _{10.3}	1073	1.070	–3.60	LD	1348–1434	± 0.6
Al ₈₇ Ni ₁₃	1123	0.847	–0.85	LD	1173–1273	± 0.5
Al _{76.5} Ni _{23.5}	1343	1.030	–5.15	LD	1418–1476	± 0.2

Table 1 (continued)

Alloy composition, at %	Liquidus temperature T_L , K	Surface tension σ_0 at T_L , Nm^{-1}	Temperature coefficient $d\sigma/dT$, $10^{-4}Nm^{-1}K^{-1}$	Method	Measurement temperature/range, K	Experim. error, %
$Al_{75}Ni_{25}$	1398	0.906	-1.50	LD	1483–1603	± 0.3
$Al_{68.5}Ni_{31.5}$	1620	0.935	-1.60	LD	1633–1733	± 0.7
$Al_{11.4}Ni_{88.6}$	1713	1.781	-4.02	LD	1728–1783	± 0.2
(Aune et al. 2006)						
$Al_{68.5}Ni_{31.5}$	1613	0.92	-5.69	OD-EML ^g	–	–
$Al_{35}Ni_{65}$	1823	1.653	-0.101	PF	–	–
$Al_{25}Ni_{75}$	1683	1.625	-5.88	PF	–	–
(Egry et al. 2008)						
$Al_{82}Ni_{18}$	1223	1.01	-5.10	OD-EML ^g	1273–1523	5.0
Al_3Ni	1383	1.21	-8.30	OD-EML ^g	1323–1723	5.0
$Al_{70}Ni_{30}$	1556	1.15	-8.80	OD-EML ^g	1573–1673	5.0
Al_3Ni_2	1832	1.30	-6.30	OD-EML ^g	1673–1973	5.0
$AlNi$	1911	1.44	-6.70	OD-EML ^g	1873–1973	5.0
$Al_{37}Ni_{63}$	1813	1.55	-2.90	OD-EML ^g	1773–2023	5.0
$AlNi_3$	1658	1.44	-2.50	OD-EML ^g	1623–1823	5.0
$Al_{13}Ni_{87}$	1706	1.58	-5.10	OD-EML ^g	1623–1873	5.0
(Egry ¹ et al. 2010a)						
$Al_{68.5}Ni_{31.5}$	1603	0.94	-1.60	R (SD; OD-EML ^{$\mu-g$})	1600–1800	–
Al_3Ni	1398	0.91	-1.50	R (SD; OD-EML ^g ; OD-EML ^{$\mu-g$})	1400–1800	–
(Brillo and Kolland 2016)						
Al	934	0.866	-1.46	OD-EML ^g	1050–1550	± 3.5
(Kobatake et al. 2015)						
Al	933	0.979	-2.71	OD-EML ^g	1310–1550	± 5.0
(Brillo and Egry 2005)						
Ni	1727	1.77	-3.30	OD-EML ^g	1423–1963	–
(Wunderlich and Fecht 2011)						
$Al_{68.5}Ni_{31.5}$	1606	1.01	-2.86	OD-EML ^{$\mu-g$}	1600–2035	± 1.1
$Al_{68.5}Ni_{31.5}$	1606	0.96	-1.96	PF	1493–1833	± 3.0
Al_3Ni	1398	0.92	-1.40	OD-EML ^{$\mu-g$}	1600–2000	± 1.4
(Fecht and Wunderlich 2017)						
Al_3Ni	1398	0.93	-1.38	PF	1323–1713	–
(Thermolab Report, ESA MAP AO-99-022, September 2007)						
$AlNi$	1896	1.341	-5.58	PF	–	–
(Thermolab Final Report, ESA MAP AO-99-022, 2006)						
Ni	1728	1.71	-2.28	PF	–	–

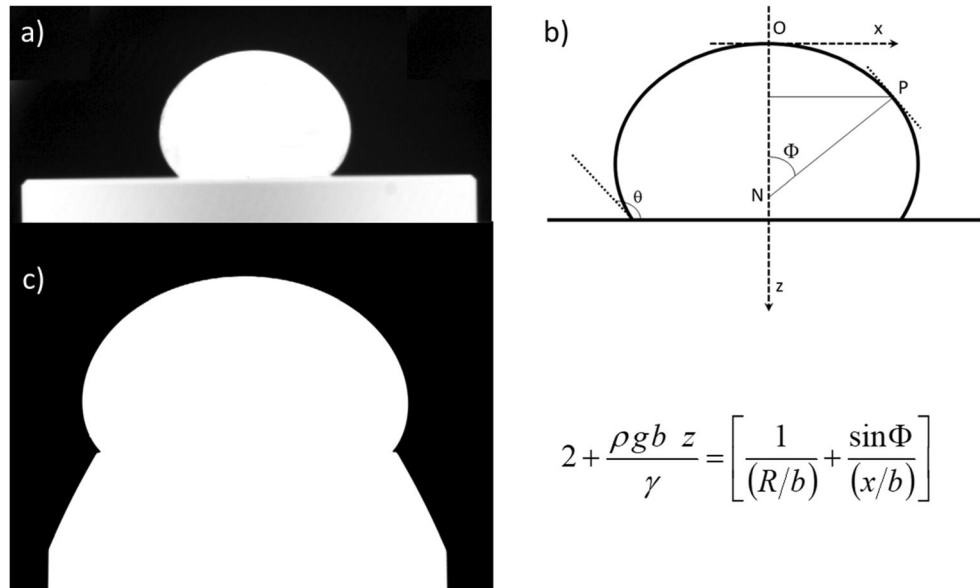
$$*\sigma = \sigma_0 - d\sigma/dT \cdot T [^\circ C]$$

Ground based (1g) EML experiments (Brillo¹ et al. 2006a) are performed in a standard stainless steel high vacuum chamber filled with He (6 N) having a pressure of $p = 8 \cdot 10^4$ Pa and/or Ar (6 N) after prior evacuation to base pressures of approximately 10^{-2} Pa.

The ≈ 4 mm large samples are positioned in the levitation coil producing the high frequency inhomogeneous electro-

magnetic field. Heating and positioning are not decoupled in the ground-based experiments and convective counter-cooling in a laminar flow of the inert gas is needed in order to adjust the desired temperature. The temperature is measured by a pyrometer focused at the sample from the side with the emissivity being estimated from the known liquidus temperature, see (Brillo² et al. 2006b).

Fig. 1 Surface tension measurements by contact methods: **a** sessile and **b** large drops with **c** equilibrium drop profile described by fitting equation (Bashforth and Adams 1883)



In 1g-EML, the symmetry of the sample is reduced as compared to an almost spherical droplet under micro gravity. This leads to a split up of the $l = 2$ Rayleigh oscillation mode into a set of five frequencies ω_m with $m = -2, -1, 0, 1, 2$. They are identified from the frequency spectra of the radius vs. time signal obtained from an image analysis of 4096 images recorded with a framerate of 400 frames per second (fps). The surface tension σ is then determined using the formula of Cummings and Blackburn (Cummings and Blackburn 1991).

$$\sigma = \frac{3M}{160\pi} \left(\sum_{m=-2}^2 \omega_m^2 - 9.5\Omega^2 - 1.5 \left(\frac{g}{a} \right)^2 \Omega^{-2} \right) \quad (1)$$

Here, M is the mass of the sample, a is its radius, and g is the gravitational acceleration. The parameter Ω corrects for the magnetic pressure. It is calculated from the three translational frequencies $\omega_x, \omega_y, \omega_z$ corresponding to the horizontal and vertical motion of the center of mass of the sample: $\Omega^2 = 1/3(\omega_{2x} + \omega_{2y} + \omega_{2z})$. The relative error $\Delta\sigma/\sigma$ in this procedure is about 5% (Brillo¹ et al. 2006a).

Oscillating Drop Method in $\mu - g$ (OD-EML ^{$\mu - g$})

Under microgravity conditions, the necessary positioning forces on the sample are strongly reduced (roughly by a factor 1000). Furthermore, the positioning and heating of the sample is decoupled, which allows the access of larger temperature ranges and removes the necessity for counter-cooling of the sample. Most importantly, the liquid drop forms a spherical shape under microgravity. Together, this suffices to fulfil the assumption of a force-free spherical sample in Rayleigh's derivation (Rayleigh 1879). As a result, the oscillation mode is not split, and consequently, under microgravity, the sub

modes $m = 0, \pm 1, \pm 2$ are degenerated and only the Rayleigh mode is visible in the spectra as a single strong peak. After Rayleigh (Rayleigh 1879), the surface tension can be obtained from the observed oscillation frequency ω of the $l = 2$ mode (Basaran 1992; Mashayek and Ashgriz 1998), for a non-viscous, force-free, spherical drop as

$$\sigma = \frac{3}{16\pi} M \omega^2 \quad (2)$$

Deviations from Rayleigh's theory are observed for strong sample rotations (Busse 1984; Mohr¹ et al. 2019a), as well as for large oscillation amplitudes (Tsamopoulos and Brown 1983; Xiao et al. 2018) or very strong damping (Reid 1960; Chandrasekhar 1981; Lohöfer 2020).

EML– Tempus/Parabolic Flights

In this study was used the Parabolic Flight airplane operated by Novespace as microgravity platform. The measurements were performed in the electromagnetic levitation facility TEMPUS ('Tiegelfreies elektromagnetisches Prozessieren unter Schwerelosigkeit', engl. 'Containerless electromagnetic processing under weightlessness') on board several parabolic flights. The facility, operated by the "Institute of Materials Physics in Space" of the German Aerospace Center, DLR is described in the literature, e.g. by Lohöfer et al. (1991). Hence, we limit the description to the necessary minimum. TEMPUS consists of a process and sample chamber, which are connected to a vacuum pumping system and gas supply unit. The sample is heated and positioned by two superimposed *rf* electromagnetic fields. A quadrupole (150 kHz) is used for positioning the sample, while a *rf* dipole

field (375 kHz) is used to heat the sample. The process chamber is furthermore equipped with two high-speed cameras that monitor the sample oscillations from two perpendicular directions. A pyrometer is integrated into the axial camera, to monitor and record the sample temperature in the range between 573 and 2373 K. The sample chamber contains the samples, loosely confined in ceramic sample holders. A mechanism allows changing samples between parabolas.

Within the 20 s microgravity duration of a parabola, the sample is preheated and positioned using the positioner field (1), then heated (2), molten (3), overheated (4) and finally cooled down (5) until solidification (6) occurs. A typical temperature-time diagram is shown in Fig. 2.

heater control voltage (blue), acceleration in units of g (green)

Within the nearly force free cooling time (5), surface oscillations are excited by applying a heater pulse. The surface oscillations are then observed using the high-speed cameras and the oscillation frequency is obtained from an edge finding algorithm and further data analysis.

Modelling

The surface properties of liquid Al-Ni alloys were analysed by three models: the Compound Formation Model (CFM), Quasi Chemical Approximation (QCA) for regular solution and Butler's model. Generally, a *bulk-surface model* is defined if its structure and energetics are known. The abovementioned models are based on the concepts of a layered interfacial structure and the energetics is expressed in terms of the thermodynamic potentials. At the interface, which is often simplified to a monolayer or to a homogeneous layer with a small limited and not further specified thickness, the bulk and the surface phases are in equilibrium with each other. The energetics of

the surface phase is expressed by that of the bulk in terms of the reduced coordination.

The Compound Formation Model (CFM) describes the surface properties of strongly interacting compound forming systems such as liquid Al-Ni alloys, most appropriately, and it includes the effects of short range ordering on these properties. It has been developed in the framework of statistical mechanics in conjunction with the quasi-lattice theory (QLT) and classical thermodynamics (Guggenheim 1952; Bhatia and Hargrove 1974). The CFM calculation of the surface tension and surface segregation isotherms of liquid Al-Ni alloys takes into account the AB-stoichiometry of the AlNi intermetallic compound, which is postulated to be energetically favoured (Ansara et al. 1997; Wang et al. 2004; Egry² et al. 2010b). The QCA for regular solution has been developed in the same framework and its numerical treatment corresponds to the calculation of a partition function for an ensemble similar to that for the CFM (Guggenheim 1952; Fowler and Guggenheim 1960; Costa et al. 2014), while the Butler model is a purely thermodynamic one (Korozs and Kaptay 2017). The surface tension isotherm calculated by the QCA is very close or even overlapping with that obtained by the Butler model and both models are properly used to describe the surface properties of weakly interacting systems. Both models can be used together with the CFM to evaluate the effects of short range ordering on the surface properties of strongly interacting systems (Egry² et al. 2010b). The difference between the surface tension values calculated by the CFM and those obtained by the QCA for regular solution (or by Butler's model) represents the contribution of short range ordering to an increase in the surface tension. An opposite effect of short range ordering on the surface segregation takes place (Novakovic and Zivkovic 2005; Novakovic and Tanaka 2006). Detailed mathematical formalisms of the CFM, QCA and Butler's model can be found elsewhere (Egry² et al. 2010b). In the following, each model is shortly described and only the equations used for the calculations are given.

Compound Formation Model (CFM)

An $A-B$ binary alloy containing N atoms of which NC and $N(1-C)$ are the numbers of A and B -atoms, in the case of compound forming systems with an $A_\mu B_\nu$ energetically favoured intermetallic phase, can be considered as a pseudoternary mixture. Indeed, taking into account the conservation of atoms, in such melts there are three types of species that are all in chemical equilibrium with one another, i.e. A and B -atoms as well as $A_\mu B_\nu$ complexes. The number of complexes n_3 is related to the constituent atoms A and B by

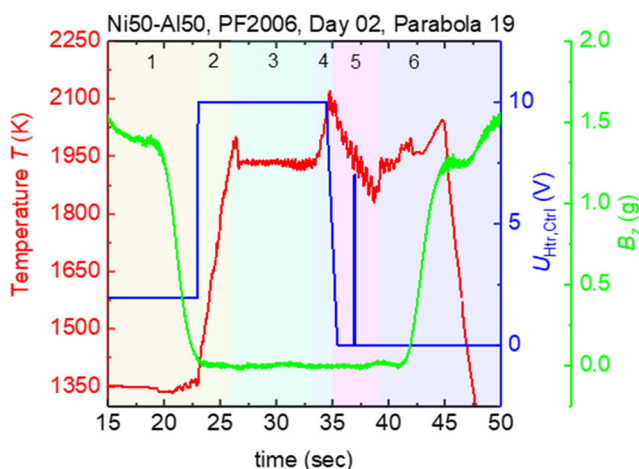


Fig. 2 Temperature-Time Diagram of a typical parabola. On the left ordinate, temperature (red), right ordinate

$$n_1 = NC - \mu n_3 \quad n_2 = N(1-C) - \nu n_3 \quad N$$

$$= n_1 + n_2 + n_3(\mu + \nu) \quad (3)$$

with N , C , $(1-C)$, μ and ν denoting the Avogadro number, atomic concentrations and stoichiometric coefficients of A and B alloy components, respectively. In the framework of CFM, the functional form of the Gibbs free energy of mixing G_M is fitted to the experimental data (the enthalpy of mixing and activities) to obtain four interaction energy parameters and subsequently, for a given temperature and pressure, minimizing the Gibbs free energy of mixing, n_3 can be calculated. Once unknown model parameters mentioned above are determined, the surface tension σ can be calculated from the relation between the bulk ($C = c_A$; $1-C = c_B$) and surface ($C^s = c_A^s$; $1-C^s = c_B^s$) compositions, as

$$\sigma = \sigma_A + \frac{k_B T}{\alpha} \ln \frac{c_A^s}{c_A} + \frac{k_B T}{\alpha} \ln \frac{\gamma_A^s}{\gamma_A} \quad (4)$$

$$\sigma = \sigma_B + \frac{k_B T}{\alpha} \ln \frac{c_B^s}{c_B} + \frac{k_B T}{\alpha} \ln \frac{\gamma_B^s}{\gamma_B} \quad (5)$$

where k_B , α , σ_i , γ_i , γ_i^s ($i = A, B$) are the Boltzmann constant, mean surface area, surface tensions, activity coefficients of the bulk and the surface phase of the pure components, respectively (Bhatia and Hargrowe 1974; Novakovic et al. 2005; Novakovic and Tanaka 2006).

QCA for Regular Solution

Thermodynamic and surface properties of simple alloy systems such as those characterised by a lens shape or eutectic type phase diagrams can be properly described by the quasi chemical approximation (QCA) for regular solution (Novakovic and Zivkovic 2005; Costa et al. 2014). This model can also be applied to the surface properties of more complex liquid alloys, but a comparison between the predicted and experimental values indicates a larger difference. Concerning the two limiting cases of a strong exothermic mixing and demixing (phase separation) in liquid binary alloys, for the calculations of their surface properties, the CFM and SAM (Self-association model), respectively, give the best results (Egry² et al. 2010b). In such systems, the presence of heterocoordinated complexes or homocoordinated clusters in alloy melts, at least near the melting points (Steeb et al. 1984; Brillo³ et al. 2006c), lead to a significant increase or decrease in the surface tension, respectively, while the surface segregation exhibits the opposite trend. For both classes of alloys, to evaluate the effects of short range

ordering or clustering on their surface properties, the QCA together with the CFM or SAM can be used. In the present work, an estimate of these effects, expressed as a difference between the property values of liquid Al-Ni alloys calculated by the CFM and QCA (Egry² et al. 2010b), will be addressed.

The QCA for regular solution is characterised by one energy parameter ω that can be calculated as a function of temperature using thermodynamic data. In the framework of QCA, the surface tension is calculated by

$$\sigma = \sigma_A + \frac{k_B T(2-pZ)}{2\alpha} \ln \frac{C^s}{C}$$

$$+ \frac{Zk_B T}{2\alpha} \left[p \ln \frac{(\beta^s - 1 + 2C^s)(1 + \beta)}{(\beta - 1 + 2C)(1 + \beta^s)} - q \ln \frac{(\beta - 1 + 2C)}{(1 + \beta)C} \right] \quad (6)$$

$$\sigma = \sigma_B + \frac{k_B T(2-pZ)}{2\alpha} \ln \frac{(1-C^s)}{(1-C)}$$

$$+ \frac{Zk_B T}{2\alpha} \left[p \ln \frac{(\beta^s + 1 - 2C^s)(1 + \beta)}{(\beta + 1 - 2C)(1 + \beta^s)} - q \ln \frac{(\beta + 1 - 2C)}{(1 + \beta)(1-C)} \right] \quad (7)$$

where Z is the coordination number, p and q are the surface coordination fractions defined as the fractions of the total number of nearest neighbours of an atom in its own layer and that in the adjoining layer. Therefore, $p + q = 1$. For a closed-packed structure, the values of these parameters usually are taken as $1/2$ and $1/4$, respectively (Costa et al. 2014). The auxiliary variable β is expressed by

$$\beta = \left[4C(1-C) \exp\left(\frac{2\omega}{Zk_B T}\right) + (1-2C)^2 \right]^{1/2} \quad (8)$$

β^s is also obtained by Eq. (8) replacing the bulk concentration C by the surface concentration C^s . The names of other variables and the associated parameters of Eqs. (6)–(8) are already known (Eqs. (3)–(5)).

Butler's Model

Butler's model has been developed in the framework of thermodynamics and, similarly to the QCA for regular solution, it is appropriate to calculate the surface tension of alloy systems with weak and moderate interactions between the constituent atoms. As stated above, the surface phase is assumed to be a monolayer and it is in equilibrium with the bulk. Using the Butler model, the surface tension of liquid binary alloys can be calculated by

$$\sigma = \sigma_i + \frac{RT}{S_i} \ln \left(\frac{C_i^s}{C_i^b} \right) + \frac{1}{S_i} \left[G_i^{xs,s}(T, C_i^s) - G_i^{xs,b}(T, C_i^b) \right] \quad (9)$$

$(i = A, B)$

where R , S_i , C_i^b , C_i^s , $G_i^{xs,b}$, $G_i^{xs,s}$ are gas constant, surface area, composition and partial excess Gibbs free energy of a component i in the bulk and surface phases, respectively. The last two mentioned are the functions of temperature and composition. From an energetic point of view, the partial excess Gibbs free energy $G_i^{xs,s}$ of the surface phase has the same functional form as that of $G_i^{xs,b}$ times a factor taking into account the reduced coordination. This factor is expressed as the ratio of the numbers of interactive contacts between neighbouring atoms in the two phases (Egry³ et al. 2010c; Korozs and Kaptay 2017). The surface properties calculated by the Butler model are very close or even overlapping with those obtained by the QCA for regular solution. In the case of ternary alloys, a comparison of experimental data with model predicted surface tension values obtained by the Butler and geometric models indicates that the results obtained by the Butler model exhibit better agreement (Egry² et al. 2010b; Costa et al. 2014). Concerning multicomponent alloys, increasing the number of components, the numerical solution of Butler's equation becomes more complex and recently, based on it, more simple approaches were reported (Duan and Guo 2020; Ferreira and Garcia 2020).

Results

The available surface tension experimental data, reported in the last 60 years, in particular those obtained in the frameworks of the EU FP6-IMPRESS, ESA-MAP Thermolab and ESA-MAP ThermoProp Projects are here collected and discussed from two points of view: experimental methods and theoretical models.

Surface Tension Data and Container-Based Methods

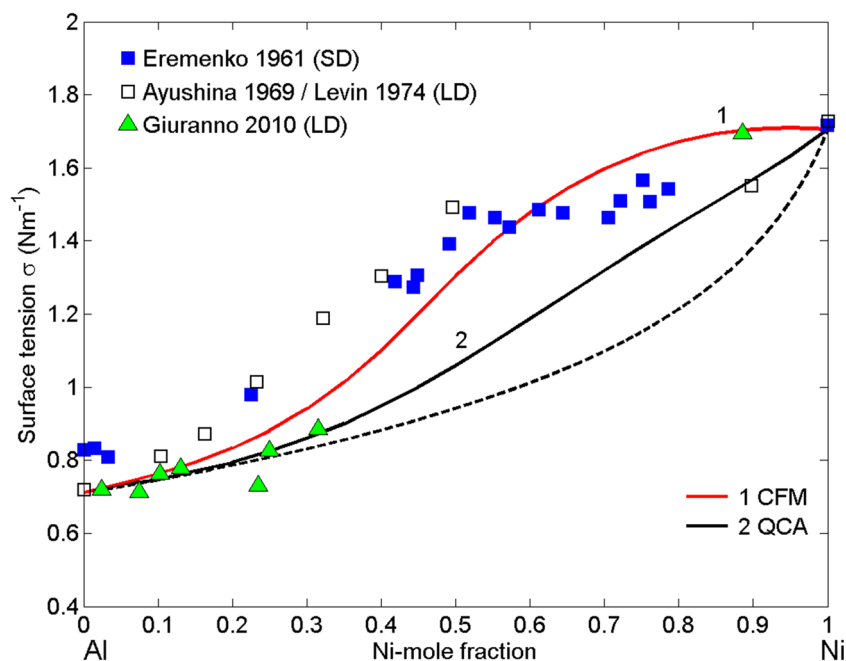
There are four surface tension datasets of liquid Al-Ni alloys obtained by container-based methods (Fig. 1). Although many details have been omitted, it is worthwhile to mention the pioneer work of Eremenko et al. in experimental determination of the surface tension of high melting alloys such as Al-Ni (Eremenko et al. 1961). The surface tension of 17 Al-Ni alloys including the pure components Al and Ni has been measured by the sessile drop method (SD) at $T = 1913$ K using polycrystalline alumina crucibles (Table 1). The measurements have been performed over entire composition range, but under different atmospheres. Indeed, the alloy compositions

containing up to 41.5 % Al have been measured in vacuum, otherwise the measurements have been conducted in a helium atmosphere. The calculated surface tension isotherm has been substantiated by these experimental data. Weight loss of about 1% was observed for intermediate and Ni-rich alloy compositions, while this value was higher for Al rich alloys processed in vacuum. Subsequently, the wetting experiments have been carried out with the aim to test the reactivity of Al-Ni liquid alloys in contact with alumina substrate. The contact angle values of Al-rich alloys were lower than 90° and together with Al absorption at the grain boundaries in Al_2O_3 indicate that the surface tension data reported in (Eremenko et al. 1961) are not reliable. At that time, Eremenko et al. have analysed the surface tension and contact angle datasets suggesting that the large drop (LD) method is more appropriate for the Al-Ni system. Indeed, after few years, the large drop method has been used to perform the measurements on seven Al-Ni alloys and pure Ni over a temperature range of 1273–2023 K (Ayushina et al. 1969). The same authors (Levin and Ayushina, 1974) have re-measured the surface tension of the same alloy compositions at $T = 1913$ K (Fig. 3), under the same experimental conditions, confirming their previous results (Table 1). Unfortunately, for the aforementioned experiments (Eremenko et al. 1961; Ayushina et al. 1969; Levin and Ayushina, 1974) detailed experimental information, in particular that on the oxygen partial pressure, are missing. Therefore, it is impossible to reproduce those experiments.

Aiming to compensate the lack or paucity of reliable surface tension data of liquid Al-Ni alloys, in the frameworks of the EU FP6-IMPRESS, ESA-MAP Thermolab and ThermoProp Projects, the experimental research of this property has been conducted by combining conventional surface tension measurements with advanced containerless processing technique that was also adopted under reduced gravity conditions. At the same time, suitable predictive models were developed and subsequently validated with the obtained experimental data. In order to identify potential sources of systematic error and to arrive at best-agreed-upon values, round-robin measurements of the same property in different laboratories and with different methods or equipment have been performed. In the case of conventional methods, the choice of an appropriate inert crucible/substrate material as well as the choice of suitable environmental atmosphere are preeminent issues to obtain reliable data.

It is important to mention that thermodynamic analysis of the systems involved together with the selection of inert or highly resistant ceramic materials with respect to the melts being investigated, and subsequent wetting tests of candidate refractory materials to identify the most promising one for the target application represent the first step of a well-assessed experimental procedure (Nowak et al. 2010). The latter issue is of particular importance to significantly reduce or even prevent contamination of a melt resulting in improved reliability

Fig. 3 Surface tension experimental data of Liquid Al-Ni alloys obtained by container-based methods: (SD)-Sessile drop and (LD)-Large drop at $T = 1923$ K together with the surface tension isotherms calculated for the same temperature (1-Compound formation model, 2-Quasi chemical approximation for regular solution, – the ideal solution model)



of experimental data. Thermodynamic and kinetic data of the Al-Ni system indicate that oxidation-evaporation phenomena are favoured in the liquid phase, in particular for Al-rich alloys, while the wetting tests performed on alumina and zirconia suggested the last one, as the best choice. Indeed, using ZrO_2 in an under-stoichiometric state, only negligible interactions with alloy melts were observed. The first experiments in pure Argon with $p_{O_2} < 10^{-18}$ Pa followed by SEM/EDS analyses of solidified alloy samples indicated a high oxygen concentration on the surface of the samples and thus, the necessity to further reduce the oxygen content. To this aim, during the surface tension measurements of all Al-Ni liquid alloys investigated, the atmosphere obtained by the combined action of $Ar-5\% H_2$ mixture with $p_{O_2} < 10^{-21}$ Pa and a Zr-getter was imposed. Under these operating conditions the measurements of a few Al-rich alloys and one Ni-rich alloy over a short temperature range were performed (Fig. 3). Some results obtained for a series of Al-Ni alloys have been reported in (Aune et al. 2006). Later, the surface tension measurements of the same alloy compositions were repeated including new Al-Ni alloys and the details of that experimental work are given in (Giuranno et al. 2010) together with the surface tension data (Table 1).

Surface Tension Data and Containerless Measurements

The experimental difficulties in handling and processing of liquid Al-Ni alloys related to container based measurement methods have been overcome by using containerless processing techniques that have been developed and well assessed in the framework of the abovementioned projects.

The surface tension data were obtained using the oscillating drop method with electromagnetic levitation ($OD-EML$), both on ground ($OD-EML^g$), and in microgravity experiments on parabolic flights (PF) or on board of sounding rockets ($OD-EML^{\mu-g}$). For metallic melts, electromagnetic levitation is a well-suited containerless technique, so the advantages of containerless processing under microgravity conditions became clear. Moreover, the reduction of the levitation forces in microgravity either leads to a significant improvement of the accuracy or makes it possible to measure highly reactive melts, such as Al-Ni.

The surface tension of Raney type Al-Ni alloy (Aune et al. 2006) followed by eight Al-Ni alloys (Egry et al. 2008) and their pure components Al (Kobatake et al. 2015) and Ni (Brillo and Egry 2005) was measured over a wide composition and temperature range using $OD-EML^g$ (Table 1). This method allows a much wider temperature range as an undercooled state is easily achieved. Among the selected alloys of particular interest were those with the compositions of intermetallic phases, because the ordering phenomena may significantly affect the surface tension.

Parabolic flights provide about 20 s of reduced gravity of which typically 10 s are in the liquid state. For many metallic alloys with the melting temperature ranging between 1273 and 2273 K, this time is sufficient for a specimen to melt, heat into the liquid phase, and cool to solidification. During the free cooling phase with the heater field turned off magnetic field pulses are applied for the excitation of surface oscillations. Within the last 15 years, many PF experiments have been performed on Al-Ni liquid alloys, and the surface tension of six alloy compositions including pure Ni was measured over the entire composition range and wide temperature ranges

(Table 1). Indeed, the surface tension data of two Al-rich alloys (Wunderlich and Fecht 2011; Fecht and Wunderlich 2017), the AlNi intermediate composition (Thermolab Report 2007), two Ni-rich alloys (Aune et al. 2006) and liquid Ni (Thermolab Final Report 2006), data were evaluated and well-assessed (Fig. 4).

The OD-EML device can improve performance when used on a sounding rocket flight ensuring cleaner liquid metal surfaces with respect to other methods. In the framework of the IMPRESS Project (IMPRESS Final Report 2009), the surface tension measurements of two Al-rich alloys containing 68.5 and 75 at % Al (Fig. 4) and over a temperature range of about 400 K were performed on a TEXUS sounding rocket flight (Table 1). In the case of Raney-type Al-Ni alloy, TEXUS sounding rocket provided about 320 s of reduced gravity of which 150 s were available for the experiments (Wunderlich and Fecht 2011).

Surface Tension Isotherms

The calculation of the surface tension isotherm by the CFM involves three steps: the selection of thermodynamic, thermophysical and structural input data; determination of order energy parameters and number of clusters, while in the case of the QCA for regular solution and Butler's model only the two first steps are necessary.

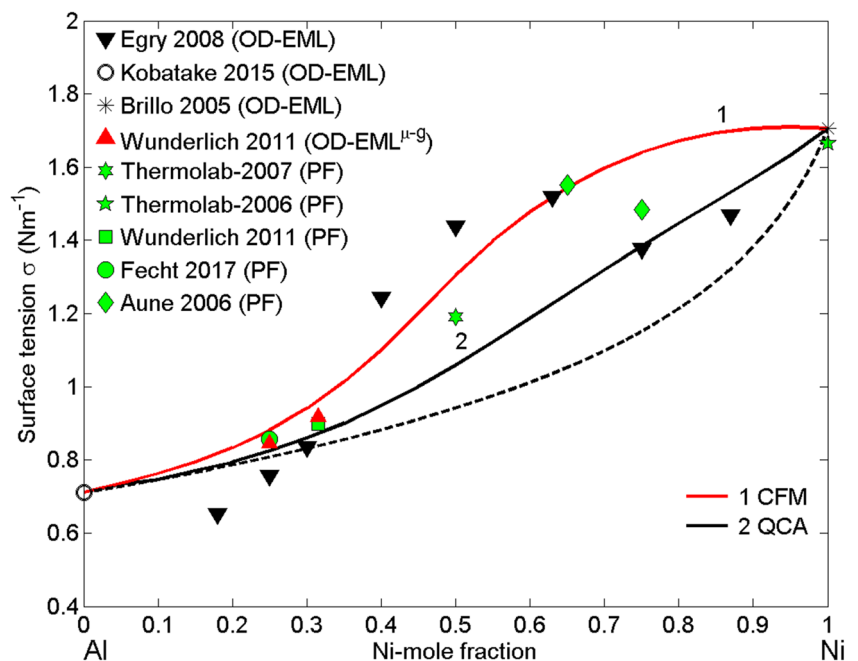
Thermodynamic Input Data

The Al-Ni phase diagram is well established and shows the presence of five intermetallic phases in the solid state, i.e. Al_3Ni , Al_3Ni_2 , Al_3Ni_5 , $AlNi$ and $AlNi_3$ of known structures

(Ansara et al. 1997; Dupin et al. 2001) suggesting short range ordering in the liquid phase (Singh and March 1995; Brillo³ et al. 2006c). A comparison of the standard enthalpies of formation of Al-Ni intermetallics shows that the $AlNi$ ($\mu = 1, \nu = 1$) is energetically favoured (Nash and Kleppa 2001; Chrifi-Alaoui et al. 2004) and therefore, in the liquid phase, the prevalence of $AlNi$ dimers is assumed Egry³ et al. 2010c). The CFM functional form of the integral Gibbs free energy of mixing (Novakovic et al. 2005; Novakovic and Tanaka 2006; Egry³ et al. 2010c) is fitted to the thermodynamic data on the enthalpy of mixing (Sandakov et al. 1971; Sudavtsova et al. 1990), Al and Ni activities (Lee and Sommer 1985; Johnson and Palmer 1980) as well as optimized data set of the excess Gibbs free energy of mixing (Ansara et al. 1997), giving four interaction energy parameters (in RT units) for $T = 1923$ K, $g = 4.52$, $\omega_{12} = -2.02$, $\omega_{13} = -2.43$, and $\omega_{23} = -2.18$. Subsequently, taking into account Eq. (3) the number of n_3 ($AlNi$ dimers), n_1 (Al) and n_2 (Ni) constituent atoms are calculated. The concentration dependence of the equilibrium values of chemical complexes n_3 exhibits the symmetry around the equiatomic composition, with the maximum value of about 0.375 (Fig. 5). With an increase in temperature, the interatomic forces become weaker and the number of n_3 decreases.

Thermodynamic data on the excess Gibbs free energy of the liquid Al-Ni phase (Ansara et al. 1997) were used as input data for the calculations of the surface tension isotherms by using the QCA for regular solution or Butler's models resulting in the overlapping curves (Egry² et al. 2010b). Taking into account that both alloy components Al and Ni have the same crystal structure (fcc), the coordination numbers Z of the bulk and surface phases are 12 and 9, respectively.

Fig. 4 Surface tension experimental data of Liquid Al-Ni alloys obtained by containerless methods: (OD-EML^g) - Electromagnetic levitation and the oscillating drop technique on ground, (PF)-Parabolic flights and (OD-EML^{μ-g}) - Electromagnetic levitation on board sounding rockets at $T = 1923$ K together with the surface tension isotherms calculated for the same temperature. (1- Compound formation model, 2- Quasi chemical approximation for regular solution, - the ideal solution model)



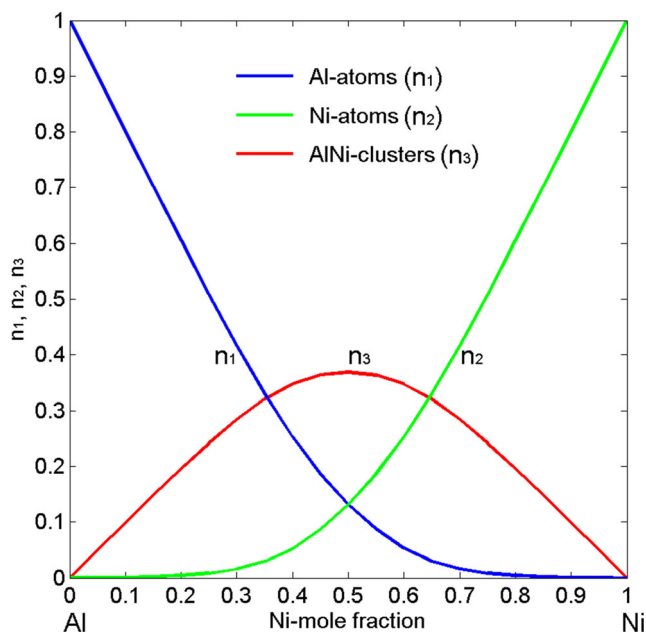


Fig. 5 Concentration dependence of equilibrium number of complexes n_3 (AlNi) together with unassociated atoms n_1 (Al) and n_2 (Ni) for liquid Al-Ni alloys calculated by the CFM for $T = 1923$ K

Accordingly, for a close packed structure of Al-Ni alloys, the surface coordination parameters are $p = 1/2$ and $q = 1/4$ (Guggenheim 1952). In all calculations the surface area of Al and Ni pure components are obtained from their molar volumes reported in (Iida and Guthrie 1993).

Surface Properties: Surface Segregation and Surface Tension

Model predicted values are directly dependent on input datasets and thus, for liquid Al-Ni alloys, reliable surface property data are necessary. High reactivity and vaporization of Al and high melting temperature of Ni make the choice of the surface tension reference data somewhat critical. It depends on the processing conditions and in particular, on the presence of oxygen in the surrounding atmosphere as well as in sample materials.

Recently, the oscillating drop method in combination with electromagnetic levitation was used to measure the surface tension of liquid Al and the obtained data together with available literature data were analysed (Kobatake et al. 2015; Brillo and Kolland 2016). The surface tension data obtained within the temperature range of 1050–1550 K can be described (Brillo and Kolland 2016) by

$$\sigma(T) = (0.866 \pm 0.03) N m^{-1} - (1.46 \pm 0.4) \cdot 10^{-4} N m^{-1} K^{-1} (T - 934 K) \quad (10)$$

They are close to 14 datasets listed in (Brillo and Kolland 2016). On the contrary, the same type of measurements

performed under an estimated surface oxygen partial pressure of 10^{-26} Pa and over a smaller temperature range of 1310–1550 K (Kobatake et al. 2015) resulted in much higher surface tension values of liquid Al (Eq. (11)) over the above-indicated temperature intervals.

$$\sigma(T) = (0.979 \pm 0.05) N m^{-1} - (2.71 \pm 0.218) \cdot 10^{-4} N m^{-1} K^{-1} (T - 934 K) \quad (11)$$

The surface tension reference data Eq. (11) shows good agreement with the data measured by Molina et al. (Molina et al. 2007) under oxygen reduced conditions. To minimize the differences between the model predicted and experimental values it is recommended to use, if possible, the input reference data obtained in the same apparatus under the same experimental conditions. Accordingly, the analysis of recently reported surface tension data of liquid Ni (Werkovits et al. 2020) including an overview of Mills and Su (Mills and Su 2006) indicate the data measured by Brillo and Egry (2005) as the most appropriate (Eq. (12)) to be used with that of liquid aluminum (Eq. (11)) as the input data for the present calculations.

$$\sigma(T) = 1.77 N m^{-1} - 3.3 \cdot 10^{-4} N m^{-1} K^{-1} (T - 1727 K) \quad (12)$$

The surface segregation and surface tension of liquid Al-Ni system were calculated as functions of bulk composition for $T = 1923$ K by using the two models: the CFM (Eqs. (4) and (5)), assuming the formation of AlNi-dimers in the liquid phase and the QCA for regular solution (Eqs. (6) and (7)). The calculated values of surface composition suggest the segregation of Al-atoms to the surface over the whole concentration range and agree with the fact that the degree of segregation decreases with an increase in temperature (Fig. 5).

The contribution of the short range ordering to the segregation of Al-atoms on the surface of Al-Ni melts was estimated by the difference in the surface composition calculated by the two models. As it is shown (Figs. 5 and 6), the presence of associates or clusters in the liquid phase significantly decreases Al-segregation, as in the case of other strong interacting systems, such as the Au-Sn or Al-Co (Novakovic and Zivkovic 2005; Novakovic and Tanaka 2006).

Once the surface segregation is obtained, it is easy to calculate the CFM and QCA surface tension isotherms inserting the corresponding surface composition values into Eqs. (4) or (5) and Eqs. (6) or (7), respectively. The calculations of the surface tension isotherms including that for the ideal solution are performed for $T = 1923$ K. The clustering effects on the surface tension and surface segregation are reciprocal, and thus the surface tension isotherm obtained by the CFM is higher than that calculated by the QCA (Figs. 3 and 4), in agreement with the

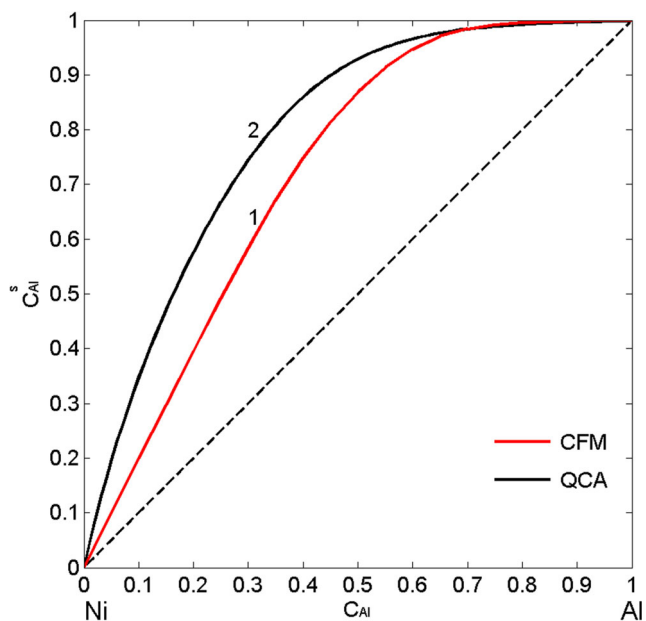
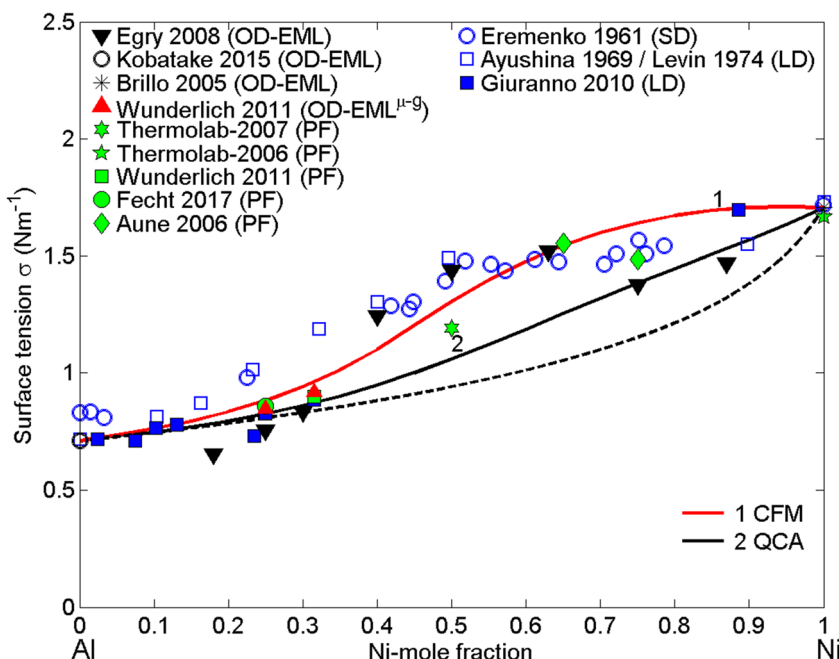


Fig. 6 Surface composition (C_{Al}^s) vs. bulk composition (C_{Al}) for liquid Al-Ni alloys calculated by the CFM (curve 1) and the QCA (curve 2) for $T = 1923\text{ K}$

previous considerations related to Al-segregation on the surface of Al-Ni melts (Fig. 6). The CFM surface tension isotherm exhibits strong irregularities near the compositions of intermetallic phases present in the Al-Ni system and agrees fairly well with the trend in available surface tension data (Fig. 7). The temperature dependence of the surface tension of all Al-Ni alloy compositions over measurement ranges can be well fitted with linear functions having negative surface tension temperature coefficients (Table 1).

Fig. 7 Surface tension experimental data of liquid Al-Ni alloys obtained by container-based methods (SD, LD) and containerless measurements: (OD-EML^s, PF and OD-EML^{μ-g}) at $T = 1923\text{ K}$ together with the surface tension isotherms calculated for the same temperature (1-Compound formation model, 2-Quasi chemical approximation for regular solution, - the ideal solution model)



Discussion

The two groups of surface tension datasets of liquid Al-Ni alloys obtained by container-based and containerless methods are firstly compared among themselves and with the model predicted values as shown in Figs. 3 and 4, followed by a comparison between all the available data and the calculated isotherms (Fig. 7).

The surface tension of liquid Al-Ni alloys, obtained by early measurements (Eremenko et al. 1961; Ayushina et al. 1969; Levin and Ayushina, 1974), exhibits the same behaviour over the entire composition range. Indeed, the surface tension values of Al-Ni alloy melts containing up to 50 at % Ni are significantly higher than those predicted by the CFM, followed by its almost constant values for the alloys with 55–90 at % Ni and reaching relatively high value for liquid Ni (Figs. 3 and 6). It was stated by the authors themselves, that relatively high surface tension values of Al-rich alloys may be attributed to combined effects of the vaporisation and oxidation of liquid Al leading to a change of sample compositions being enriched in Ni. On the contrary, intermediate and Ni-rich alloy compositions are less prone to the oxidation/vaporisation phenomena and their surface tension values result more realistic. More recent surface tension data of liquid Al-Ni alloys (Giuranno et al. 2010) obtained by the large drop method show good agreement with the CFM isotherm for Al-rich and Ni-rich alloys, while the data of $Al_{68.5}Ni_{31.5}$ Raney type industrial alloy and the Al_3Ni agree completely with the QCA isotherm (Fig. 3). Among Al-rich alloys, only the surface tension of the $Al_{76.5}Ni_{23.5}$ differs from the model predicted values probably due to slight oxidation of the sample. The thermodynamic and kinetic data of the Al-Ni system, SEM/

EDS analysis of the alloy samples after surface tension determination and surface tension experimental data indicate that container-based methods are not recommended for the surface tension measurements of intermediate and Ni-rich alloys. Indeed, the container is acting as substrate contributing energetically to the vaporization phenomenon. Therefore, containerless measurements result in reducing the effects of vaporisation /oxidation phenomena and are appropriate methods Al-Ni alloys with high melting temperatures.

The surface tension values of liquid Al-Ni alloys with intermediate compositions, obtained by the *OD-EML^g* method (Egry et al. 2008), agree with the CFM values, while those of Al- and Ni-rich alloys show better agreement with the QCA isotherm (Figs. 4 and 7). The surface tension data of two Al-Ni alloys with intermediate compositions, obtained by *PF* (Thermolab Final Report 2006; Aune et al. 2006), exhibit good agreement with the CFM values, while that of the *AlNi₃* (Aune et al. 2006) agrees better with the QCA value. The surface tension data of the *Al_{68.5}Ni_{31.5}* (Raney type alloy) and the *Al₃Ni* obtained by *PF* (Wunderlich and Fecht 2011; Fecht and Wunderlich 2017) agree fairly well with the corresponding values obtained by the CFM and QCA, respectively. The surface tension experimental data of the same Al-Ni alloys measured by the *OD-EML^{μ-g}* (Wunderlich and Fecht 2011) exhibit almost perfect agreement with the CFM predicted values (Figs. 4 and 7).

Generally, the surface tension data of liquid Al-Ni alloys agree with the CFM predicted values (Fig. 7) exhibiting a clear correlation between the thermodynamic and surface properties. The effects of extremely small amounts of surfactants such as oxygen have a strong influence on the surface properties of these alloys. Moreover, depending on the alloy composition, the combined effects of oxidation/vaporisation in the case of Al-rich alloys and oxidation/short range ordering favoured during melting of intermediate alloys make it difficult to predict in a rigorous manner the surface tension behaviour of Al-Ni liquid alloys.

Conclusions

Surface tension experimental datasets of liquid Al-Ni alloys obtained by container-based and containerless measurement methods were analysed by the CFM, QCA and Butler's predictive models. The CFM surface tension isotherm exhibits strong irregularities near the compositions of intermetallic phases present in the Al-Ni system and agrees fairly well with the trend in available surface tension data. The combined effects of oxidation/vaporisation in the case of Al-rich alloys and oxidation/short range ordering favoured during melting of intermediate alloys make it difficult to predict in a rigorous manner the surface tension behaviour of Al-Ni liquid alloys. For the same reasons, for the determination of their surface

tension, the containerless methods are the most appropriate. The surface tension values of the *Al_{68.5}Ni_{31.5}* (Raney type alloy) and the *Al₃Ni* obtained by the *OD-EML^{μ-g}* are the reference data for these alloys.

Acknowledgements The reported work was partially performed in the framework of the ESA-MAP project ThermoProp (AO-099-022 and AO-2009-1020).

M. M., R. W. and H.-J. F. further acknowledge funding from the DLR Space Administration with funds provided by the Federal Ministry for Economic Affairs and Energy (BMW) under Grant No. 50WM1759.

The support from the Institute of Materials Physics in Space of the DLR, Cologne in conducting the experiments during the parabolic flight campaigns and its support in experiment preparation is gratefully acknowledged.

References

- Amore, S., Valenza, F., Giuranno, D., Novakovic, R., Dalla Fontana, G., Battezzati, L., Ricci, E.: Thermophysical properties of some Ni-based superalloys in the liquid state relevant for solidification processing. *J. Mater. Sci.* **51**, 1680–1688 (2016)
- Ansara, I., Dupin, N., Lukas, H.L., Sundman, B.: Thermodynamic assessment of the Al-Ni system. *J. Alloys Compd.* **247**(1–2), 20–30 (1997)
- Ashby, M.F., Bréchet, Y.J.M., Cebon, D., Salvo, L.: Selection strategies for materials and processes. *Mater. Design.* **25**(1), 51–67 (2004)
- Aune, R., Battezzati, L., Egry, I., Etay, J., Fecht, H.J., Giuranno, D., Novakovic, R., Passerone, A., Ricci, E., Schmidt-Hohagen, F., Seetharaman, S., Wunderlich, R.: Surface tension measurements of Al-Ni based alloys from ground-based and parabolic flight experiments: results from the thermolab projects. *Microgravity Sci. Technol.* **XVIII**(3/4), 73–76 (2006)
- Ayushina, G.D., Levin, E.S., Gel'd, P.V.: The density and surface energy of liquid alloys of aluminium with cobalt and nickel. *Russ. J. Phys. Chem.* **43**(11), 1548–1551 (1969)
- Basaran, O.A.: Nonlinear oscillations of viscous liquid drops. *J. Fluid Mech.* **241**, 169–198 (1992)
- Bashforth, F., Adams, J.: An Attempt to Test the Theories of Capillary Action. Cambridge University Press, Cambridge (1883)
- Bhatia, A.B., Hargrove, W.H.: Concentration fluctuations and thermodynamic properties of some compound forming binary molten systems. *Phys. Rev. B.* **10**, 3186–3196 (1974)
- Brillo, J.: Thermophysical Properties of Multicomponent Liquid Alloys. deGruyter Oldenbourg, Berlin (2016)
- Brillo, J., Egry, I.: Surface tension of nickel, copper, iron and their binary alloys. *J. Mater. Sci.* **40**, 2213–2216 (2005)
- Brillo, J., Kolland, G.: Surface tension of liquid Al-Au binary alloys. *J. Mater. Sci.* **51**, 4888–4901 (2016)
- Brillo, J., Lohöfer, G., Schmid-Hohagen, F., Schneider, S., Egry, I.: Thermophysical property measurements of liquid metals by electromagnetic levitation. *Int. J. Mater. Prod. Tec.* **26**, 247–273 (2006a)
- Brillo, J., Egry, I., Ho, I.: Density and thermal expansion of liquid Ag-Cu and Ag-Au alloys. *Int. J. Thermophys.* **27**, 494–506 (2006b)
- Brillo, J., Bytchkov, A., Egry, I., Hennem, L., Mathiak, G., Pozdnyakova, I., Price, D.L., Thiaudiere, D., Zanghi, D.: Local structure in liquid binary Al-Cu and Al-Ni alloys. *J. Non-Cryst. Solids* **352**, 4008–4012 (2006c)
- Busse, F.H.: Oscillations of a rotating liquid drop. *J. Fluid Mech.* **142**, 1–8 (1984)
- Chandrasekhar, S.: Hydrodynamic and Hydromagnetic Stability. Dover Publications, New York (1981)

- Chrifi-Alaoui, F.Z., Nassik, M., Mahdouk, K., Gachon, J.C.: Enthalpies of formation of the Al-Ni intermetallic compounds. *J. Alloy. Compd.* **364**, 121–126 (2004)
- Cormier, J.: Ni- and Co-based superalloys and their coatings. *Metals*. **8**(1055), 1–3 (2018)
- Costa, C., Delsante, S., Borzone, G., Zivkovic, D., Novakovic, R.: Thermodynamic and surface properties of liquid Co-Cr-Ni alloys. *J. Chem. Thermodyn.* **69**, 73–84 (2014)
- Cummings, D.L., Blackburn, D.A.: Oscillations of magnetically levitated aspherical droplets. *J. Fluid Mech.* **224**, 395–416 (1991)
- De, S., Zhang, J., Luque, R., Yan, N.: Ni-based bimetallic heterogeneous catalysts for energy and environmental applications. *Energy Environ. Sci.* **9**, 3314–3347 (2016)
- Defay, R.: *Thermodynamique de la Tension Superficielle*. Gauthier-Villars, Paris (1971)
- Duan, S.-C., Guo, H.-J.: Determination of viscosity and surface tension of liquid Ni-Al-Ti system using the evaluated thermodynamic properties by AMCT. *J. Mater. Sci.* **55**, 11071–11085 (2020)
- Dupin, N., Ansara, I., Sundman, B.: Thermodynamic re-assessment of the ternary system Al-Cr-Ni. *Calphad.* **25**(2), 279–298 (2001)
- Egry, I.: Surface tension measurements of liquid metals by the oscillating drop technique. *J. Mater. Sci.* **26**, 2997–3003 (1991)
- Egry, I., Giffard, H., Schneider, S.: The oscillating drop technique revisited. *Meas. Sci. Technol.* **16**, 426–431 (2005)
- Egry, I., Brillo, J., Holland-Moritz, D., Plevachuk, Y.: The surface tension of liquid aluminium-based alloys. *Mater. Sci. Eng. A.* **495**, 14–18 (2008)
- Egry, I¹, Brooks, R., Holland-Moritz, D., Novakovic, R., Matsushita, T., Plevachuk, Yu., Ricci, E., Seetharaman, S., Sklyarchuk, V., Wunderlich, R.: Thermophysical properties of liquid Al-Ni alloys. *High Temp.-High Press.* **38**(4), 343–351 (2010a)
- Egry, I², Ricci, E., Novakovic, R., Ozawa, S.: Surface tension of liquid metals and alloys-recent developments. *Adv. Colloid. Interface Sci.* **159**, 198–212 (2010b)
- Egry, I³, Holland-Moritz D., Novakovic R., Ricci E., Wunderlich R., Sobczak N.: Thermophysical properties of liquid AlTi-based alloys. *Int. J. Thermophys.* **31**, 949–965 (2010c)
- Eremenko, V.N., Nizhenko, V.I., Naidich, Y.V.: *Izv. Akad. Nauk SSSR. Metallurgiya i Topivo.* **3**, 150–154 (1961) (in Russian)
- Fecht, H.J.: The thermoLab project: high-precision thermophysical property data of liquid metals for modelling of industrial solidification processes. *High Temp. Mater. Proc. Spec. Issue.* **27**(6), 385–388 (2008)
- Fecht, H.-J., Wunderlich, R.K.: Fundamentals of liquid processing in low earth orbit: from thermophysical properties to microstructure formation in metallic alloys. *JOM.* **69**(8), 1261–1268 (2017)
- Fecht, H.-J., Schneider, S., Wunderlich, R.K., Battezzati, L., Papandrea, C., Palumbo, M., Egry, I., Mills, K., Quested, P., Brooks, R., Giuranno, D., Novakovic, R., Passerone, A., Ricci, E., Seetharaman, S., Aune, R., Vinet, B., Garandet, J.-P.: Measurement of thermophysical properties of liquid metallic alloys in a ground- and microgravity based research program. The thermolab project. *Metallurgia Italiana.* **97**(3), 47–53 (2005)
- Ferreira, I.L., Garcia, A.: The application of numerical and analytical approaches for the determination of thermophysical properties of Al-Si-Cu-Mg alloys. *Contin. Mech. Thermodyn.* **32**, 1231–1244 (2020)
- Fowler, R.H., Guggenheim, E.A.: *Statistical Thermodynamics*. Cambridge University Press, Cambridge (1960)
- Furrer, D., Fecht, H.: Ni-based superalloys for turbine discs. *JOM.* **51**(1), 14–17 (1999)
- Giuranno, D., Tuissi, A., Novakovic, R., Ricci, E.: Surface tension and density of Al-Ni alloys. *J. Chem. Eng. Data.* **55**(9), 3024–3028 (2010)
- Giuranno, D., Amore, S., Novakovic, R., Ricci, E.: Surface tension and density of RENE N5 and RENE 90 Ni-based superalloys. *J. Mater. Sci.* **50**, 3763–3771 (2015)
- Guggenheim, E.A.: *Mixtures*, p. 271. Oxford University Press, London (1952)
- Iida, T., Guthrie, R.I.L.: *The Physical Properties of Liquid Metals*. Clarendon Press, Oxford (1993)
- IMPRESS-Intermetallic Materials Processing in Relation to Earth and Space Solidification. Integrated Project, NMP3-CT-2004-500635, Final Activity Report. 2004–2009 October 31 2009
- Jarvis, D.J., Voss, D.: IMPRESS integrated project-an overview paper. *Mater. Sci. Eng. A.* **413–414**, 583–591 (2005)
- Johnson, G.R., Palmer, L.D.: Quad-cell mass spectrometry: thermodynamic properties of liquid aluminium-nickel alloys. *High Temp. High Press.* **12**(3), 261–266 (1980)
- Keller, T., Lindwall, G., Ghosh, S., Ma, L., Lane, B.M., Zhang, F., Kattner, U.R., Lass, E.A., Heigel, J.C., Idell, Y., Williams, M.E., Allen, A.J., Guyer, J.E., Levine, L.E.: Application of finite element, phase-field, and CALPHAD-based methods to additive manufacturing of Ni-based superalloys. *Acta Mater.* **139**(15), 244–253 (2017)
- Kobatake, H., Brillo, J., Schmitz, J., Pichon, P.-Y.: Surface tension of binary Al-Si liquid alloys. *J. Mater. Sci.* **50**, 3351–3360 (2015)
- Korozs, J., Kaptay, G.: Derivation of the Butler equation from the requirement of the minimum Gibbs energy of a solution phase, taking into account its surface area. *Colloids Surf. A Physicochem. Eng. Asp.* **533**, 296–301 (2017)
- Kozakevitch, P., Urbain, G.: *Mém. Sci. Rev. Metall.* **58**, 401, p. 517, p. 931 (1961)
- Lee, J.-J., Sommer, F.: Determination of partial enthalpies of mixing of aluminum-rich alloy melts by solution calorimetry. *Z. Metallkd.* **76**(11), 750–754 (1985)
- Levin, E.S., Ayushina, G.D.: Density and surface properties of liquid Al-alloys with chromium, iron, cobalt and nickel. *Izv. Ural. Polytechn. Inst.* **231**, 93–96 (1974) (in Russian)
- Lohöfer, G.: Viscosity measurement by the “oscillating drop method”: the case of strongly damped oscillations. *Int. J. Thermophys.* **41**, 30 (2020)
- Lohöfer, G., Neuhaus, P., Egry, I.: TEMPUS – a facility for measuring thermophysical properties of undercooled liquid metals. *High. Temp. High. Press.* **23**, 333–342 (1991)
- Mashayek, F., Ashgriz, N.: Nonlinear oscillations of drops with internal circulation. *Phys. Fluids.* **10**, 1071–1082 (1998)
- Maze, C., Burnet, G.: A non-linear regression method for calculating surface tension and contact angle from the shape of a sessile drop. *Surf. Sci.* **13**(2), 451–470 (1969)
- Maze, C., Burnet, G.: Modification of a non-linear regression technique used to calculate surface tension from sessile drops. *Surf. Sci.* **24**, 335–342 (1971)
- Mills, K.C., Su, Y.C.: Review of surface tension data for metallic elements and alloys: part 1-pure metals. *Int. Mater. Rev.* **51**(6), 329–351 (2006)
- Mohr, M¹, Wunderlich, R.K., Koch, S., Galenko, P.K., Gangopadhyay, A.K., Kelton, K.F., Jiang, J.Z., Fecht, H.-J.: Surface tension and viscosity of Cu₅₀Zr₅₀ measured by the oscillating drop technique on board the international space station. *Microgravity Sci. Technol.* **31**, 177–184 (2019a)
- Mohr, M², Wunderlich, R., Dong, Y., Furrer, D., Fecht, H.-J.: Thermophysical properties of advanced Ni-based superalloys in the liquid state measured on board the international space station. *Adv. Eng. Mater.* **22** 1901228, 1–10 (2019b)
- Molina, J.M., Voytovych, R., Louis, E., Eustathopoulos, N.: The surface tension of liquid aluminium in high vacuum: the role of surface condition. *Int. J. Adh. Adhes.* **27**, 394–401 (2007)
- Naidich, Y.V.: The wettability of solids by liquid metals. In: Cadenhead, D.A., Danielli, J.F. (eds.) *Progress in Surface and Membrane Science*, pp. 353–484. Academic Press, New York (1981)

- Nandwana, P., Elliott, A.M., Siddel, D., Merriman, A., Peter, W.H., Babu, S.S.: Powder bed binder jet 3D printing of Inconel 718: densification, microstructural evolution and challenges. *Curr. Opin. Solid State Mater. Sci.* **21**(4), 207–218 (2017)
- Nash, P., Kleppa, O.: Composition dependence of the enthalpies of formation of NiAl. *J. Alloy. Compd.* **321**, 228–231 (2001)
- Novakovic, R., Tanaka, T.: Bulk and surface properties of Al-Co and Co-Ni liquid alloys. *Physica B. Condens. Matter.* **371**, 223–231 (2006)
- Novakovic, R., Zivkovic, D.: Thermodynamics and surface properties of liquid Ga-X (X = Sn, Zn) alloys. *J. Mater. Sci.* **40**, 2251–2257 (2005)
- Novakovic, R., Ricci, E., Gnecco, F., Giuranno, D., Borzone, G.: Surface properties of Au-Sn liquid alloys. *Surf. Sci.* **599**(1–3), 230–247 (2005)
- Nowak, R., Lanata, T., Sobczak, N., Ricci, E., Giuranno, D., Novakovic, R., Holland-Moritz, D., Egry, I.: Surface tension of γ -TiAl-based alloys. *J. Mater. Sci.* **45**, 1993–2001 (2010)
- Padday, F.: *Surface and Colloid Science*. Wiley-Interscience, New York (1969)
- Park, S.-J., Seo, S.-M., Yoo, Y.-S., Jeong, H.-W., Jang, H.J.: Effects of Al and Ta on the high temperature oxidation of Ni-based superalloys. *Corros. Sci.* **90**, 305–312 (2015)
- Pollock, T.M., Tin, S.: Nickel-based superalloys for advanced turbine engines: chemistry, microstructure, and properties. *J. Propuls. Power.* **22**(2), 361–374 (2006)
- Quested, P.N., Brooks, R.F., Chapman, L., Morrell, R., Youssef, Y., Mills, K.C.: Measurement and estimation of thermophysical properties of nickel based superalloys. *Mater. Sci. Technol.* **25**, 154–162 (2009)
- Rayleigh, L.: On the capillary phenomena of jets. *Proc. Royal. Soc.* **29**, 71–97 (1879)
- Reid, W.H.: The oscillation of a viscous liquid drop. *Q. Appl. Math.* **18**, 86–89 (1960)
- Ricci, E., Giuranno, D., Novakovic, R., Matsushita, T., Seetharaman, S., Brooks, R., Chapman, L., Quested, P.: Density, surface tension, and viscosity of CMSX-4 superalloy. *Int. J. Thermophys.* **28**(4), 1304–1321 (2007)
- Rösler, J., Näth, O., Jäger, S., Schmitz, F., Mukherji, D.: Fabrication of nanoporous Ni-based superalloy membranes. *Acta Mater.* **53**, 1397–1406 (2005)
- Sandakov, V.M., Esin, Y.O., Geld, P.V.: Enthalpies of formation of molten nickel-aluminum alloys at 1650°C. *Zh. Fiz. Chim.* **45**, 1798 (1971) (in Russian)
- Singh, R.N., March, N.H.: Liquid and vapour species. In: Westbrook, J.H., Fleischer, R.L. (eds.) *Intermetallic Compounds, Principles and Practice*, vol. 1, pp. 661–686. Wiley, Chichester (1995)
- Steeb, S., Falch, S., Lamparter, P.: Struktur und thermisches Verhalten rasch abgeschreckter Legierungen. *Z. Metallkd.* **75**(8), 599–613 (1984) (in German)
- Sudavtsova, V.S., Shuvalov, A.V., Sharkina, N.O.: Thermodynamic properties of liquid binary Al-Cr (Ni) alloys. *Rasplavy.* **4**, 97–99 (1990)
- Thermolab Final Report. ESA MAP Contract Number AO-99-022. 2003
- Thermolab Final Report. ESA MAP AO-99-022. 2006
- Thermolab Report. ESA MAP AO-99-022. September 2007
- Tsamopoulos, J.A., Brown, R.A.: Nonlinear oscillations of inviscid drops and bubbles. *J. Fluid Mech.* **127**, 519–537 (1983)
- Wang, Y., Liu, Z.-K., Chen, L.-Q.: Thermodynamic properties of Al, Ni, NiAl, and Ni₃Al from first-principles calculations. *Acta Mater.* **52**, 2665–2671 (2004)
- Wang, J.C., Osawa, M., Yokokawa, T., Harada, H., Enomoto, M.: Modeling the microstructural evolution of Ni-base superalloys by phase field method combined with CALPHAD and CVM. *Comput. Mater. Sci.* **39**(4), 871–879 (2007)
- Weber, J.H., Khalfalla, Y.E., Benyounis K.Y.: Nickel-based superalloys: alloying methods and thermomechanical processing. In: *BT – Reference Module in Materials Science and Materials Engineering*. Elsevier BV, (Amsterdam) Web 2016. doi: <https://doi.org/10.1016/B978-0-12-803581-8.03383-X>
- Werkovits, A., Leitner, T., Potlacher, G.R.: Surface tension of liquid nickel: re-evaluated and revised data. *High Temp.- High Press.* **49**, 107–124 (2020)
- Wunderlich, R.K., Fecht, H.-J.: Surface tension and viscosity of NiAl catalytic precursor alloys from microgravity experiments. *Int. J. Mat. Res.* **102**(9), 1164–1173 (2011)
- Wunderlich, R.K., Fecht, H.-J., Lohöfer, G.: Surface tension and viscosity of the Ni-based superalloys LEK94 and CMSX-10 measured by the oscillating drop method on board a parabolic flight. *Metall. Mater. Trans. B Process Metall. Mater. Process. Sci.* **48**, 237–246 (2017)
- Wunderlich, R.K., Hecht, U., Hediger, F., Fecht, H.-J.: Surface tension, viscosity, and selected thermophysical properties of Ti48Al48Nb2Cr2, Ti46Al46Nb8, and Ti46Al46Ta8 from microgravity experiments. *Adv. Eng. Mater.* **20**(1–9), 1800346 (2018)
- Xiao, X., Hyers, R.W., Wunderlich, R.K., Fecht, H.-J., Matson, D.M.: Deformation induced frequency shifts of oscillating droplets during molten metal surface tension measurement. *Appl. Phys. Lett.* **113**, 011903 (2018)
- Zeifert, B., Salmones Blasquez, J., Cabanas Moreno, J.G., Caldero, H.A.: Raney-nickel catalysts produced by mechanical alloying. *Rev. Adv. Mater. Sci.* **18**, 632–638 (2008)

Publisher's Note Springer Nature remains neutral with regard to jurisdictional claims in published maps and institutional affiliations.